Phytochemistry 142 (2017) 68–75

Contents lists available at ScienceDirect

Phytochemistry

journal homepage: www.elsevier.com/locate/phytochem

Bioactive polyketides and 8,14-*seco*-ergosterol from fruiting bodies of the ascomycete *Daldinia childiae*

Zhen-Zhu Zhao [a, c], He-Ping Chen [a, b], Ying Huang [a, c], Shuai-Bing Zhang [a, c], Zheng-Hui Li [b], Tao Feng [b, *], Ji-Kai Liu [b, **]

[a] State Key Laboratory of Phytochemistry and Plant Resources in West China, Kunming Institute of Botany, Chinese Academy of Sciences, Kunming 650201, People's Republic of China
[b] School of Pharmaceutical Sciences, South-Central University for Nationalities, Wuhan 430074, People's Republic of China
[c] University of Chinese Academy of Sciences, Beijing 100049, People's Republic of China

ARTICLE INFO

Article history:
Received 5 April 2017
Received in revised form
12 June 2017
Accepted 30 June 2017
Available online 4 July 2017

Keywords:
Ascomycete
Daldinia childiae
Polyketide
8,14-*Seco*-ergosterol
Anti-bacterial
Anti-NO activity

ABSTRACT

Seven previously undescribed polyketides, namely childinins A-G, and one previously undescribed 8,14-*seco*-ergosterol, namely childinasterone A, were obtained from the fruiting bodies of *Daldinia childiae*. Their structures and absolute configurations were established via extensive spectroscopic analyses, single-crystal X-ray diffraction, and TDDFT/ECD calculations. Childinins A represents the first example of natural product possessing a previously undescribed 6*H*-naphtho[2,1-*c*]chromen-6-one scaffold. The single crystal X-ray diffraction of childinasterone A unambiguously determined the absolute configuration of a 8,14-*seco*-ergosterol skeleton. Childinins A, B, F and G (MIC_{90} 54.9 $\mu g \cdot mL^{-1}$) showed anti-bacterial activities. Childinasterone A showed significant anti-NO activity (IC_{50} 21.2 μM) and weak activities against SMMC-7721, MCF-7 and SW480 cell lines.

1. Introduction

Daldinia is a genus of fungi belonging to the family Xylariaceae. This genus was considered as a talented source of polyketides with unique structures and pronounced biological activities. Concentricolide is an anti-HIV agent isolated from the fruiting bodies of *D. concentrica* with an EC_{50} value of 0.3 $\mu g \cdot mL^{-1}$ (Chang and Chein, 2011; Fang and Liu, 2009; Qin et al., 2006). The mantis associated fungus *D. eschscholzii* has long been investigated for producing skeletally unprecedented molecules, including the potent immunosuppressive agents dalesconols A and B (Zhang et al., 2008), the cell differentiation inducer selesconol (Zhang et al., 2016b), and the NLRP3 inflammasome activation inhibitor spirodalesol (Zhang et al., 2016a).

The fungus *D. childiae* has rarely been chemically investigated. To the best of our knowledge, only one article dealt with the chemical constituents of fruiting bodies of this fungus, which resulted in the isolation of three nitric oxide production inhibitors daldinals A-C (Quang et al., 2006). In the course of chemical investigation of bioactive promising and/or structurally interesting natural compounds from mushrooms, childinin A (**1**), the first natural product harboring a 6*H*-naphtho[2,1-*c*]chromen-6-one skeleton, a previously undescribed 2-phenylisobenzofuran-4,5-dione (**2**), a pair of racemic isoindolinones (**3a** and **3b**), two benzophenones (**4** and **5**), two 2*H*-pyran-2-one derivatives (**6** and **7**), and an 8,14-*seco*-ergosterol (**8**), were identified from the fruiting bodies of *D. childiae* (see Fig. 1).

2. Results and discussion

2.1. Structure elucidation of previously undescribed fungal metabolites (*1*–*8*)

Compound **1** was isolated as yellow powder. Its molecular formula was determined to be $C_{20}H_{16}O_5$ by HREIMS at *m/z* 336.1003 $[M]^+$ (calcd for $C_{20}H_{16}O_5$, 336.0998), indicating thirteen degrees of unsaturation. The UV absorption at 398 nm revealed the presence

* Corresponding author.
** Corresponding author.
E-mail addresses: tfeng@mail.scuec.edu.cn (T. Feng), jkliu@mail.kib.ac.cn, liujikai@mail.scuec.edu.cn (J.-K. Liu).

http://dx.doi.org/10.1016/j.phytochem.2017.06.020
0031-9422/

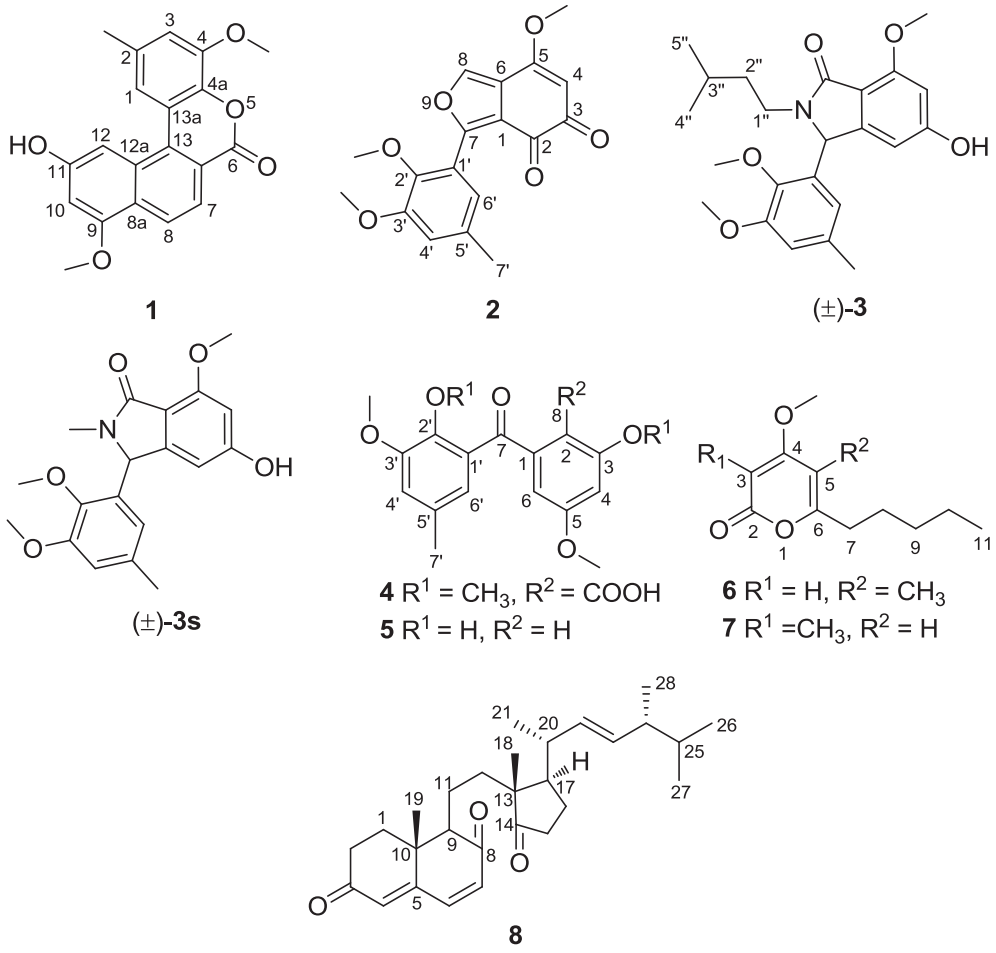

Fig. 1. Metabolites **1**–**8** isolated from the fungus *D. childiae* and simplified structure **3s** for ECD calculation.

of a highly conjugated system in **1**. The ^{1}H NMR spectrum showed clear signals for six aromatic protons, at δ 6.93 (H-3, d, J = 1.6 Hz), 7.18 (H-10, d, J = 2.0 Hz), 7.96 (H-1, d, J = 1.6 Hz), 8.27 (H-12, d, J = 2.0 Hz), 8.40 (H-7, d, J = 8.6 Hz), 8.50 (H-8, d, J = 8.6 Hz); two methoxys at δ 3.87 (4-OMe), 3.94 (9-OMe), and one methyl singlet at δ 2.12 (Me-14) (Table 1). Analysis of the 1D NMR (Table 1) and HMBC spectroscopic data (Fig. 2) delineated a tetrasubstituted naphthalene ring and a tetrasubstituted benzene ring, accounting for eleven degrees of unsaturation. Additionally, the key HMBC correlation from H-1 to C-13 indicated the connection of the naphthalene ring and benzene ring between C-13 and C-13a. Moreover, the HMBC correlation from H-7 to C-6 (δ_C 162.3), as well as the downfield-shift of C-4a and the remaining two degrees of unsaturation, suggested the assignment of an ester bond between C-6 and C-4a (Fig. 2). These evidences revealed that **1** is a naphthalene/chromone-fused polyketide which represented the first of 6*H*-naphtho[2,1-*c*]chromen-6-one scaffold as a natural example. The C-11 is substituted by a hydroxy group based on HREIMS data and chemical shifts analysis of C-10, C-11, and C-12. Thus, the structure of **1** was determined to be 11-hydroxy-4,9-dimethoxy-2-methyl-6*H*-naphtho[2,1-*c*]chromen-6-one and named as childinin A.

The molecular formula of childinin B (**2**) was determined to be $C_{18}H_{16}O_6$ (11 degrees of unsaturation) by HREIMS with *m/z* 328.0941 $[M]^+$ (calcd for $C_{18}H_{16}O_6$, 328.0947). The 1D NMR and HSQC spectra revealed the presence of one methyl (δ_H 2.34, s; δ_C 21.1), three methoxys (δ_H 3.75, 3.90, 4.04, δ_C 61.4, 56.3, 57.3), and two carbonyl carbons (δ_C 175.3, 182.3), while a 1,3,4,5-tetrasubstituted benzene (δ_H 7.07, brd, J = 2.0 Hz; 7.08, brd, J = 2.0 Hz) ring was also identified with the aid of HMBC correlations from 2′-OMe (δ_H 3.90) to C-2′ (δ_C 146.7); 3′-OMe (δ_H 3.75) to C-3′ (δ_C 153.6); 7′-Me (δ_H 2.34) to C-4′ (δ_C 117.4), C-5′ (δ_C 134.2), C-6′

Table 1
NMR spectroscopic data (600 MHz, C_5D_5N) for childinin A (**1**).

No.	δ_C, type	δ_H (J in Hz)
1	119.6, CH	7.96, d (1.6)
2	133.8, C	
3	113.7, CH	6.93, d (1.6)
4a	140.0, C	
4	148.7, C	
6	162.3, C	
6a	132.0, C	
7	121.2, CH	8.40, d (8.6)
8	124.5, CH	8.50, d (8.6)
8a	124.7, C	
9	158.2, C	
10	101.9, CH	7.18, d (2.0)
11	160.3, C	
12	103.1, CH	8.27, d (2.0)
12a	122.3, C	
13	132.9, C	
13a	120.6, C	
14	21.9, CH_3	2.12, s
4-OMe	56.6, CH_3	3.87, s
9-OMe	56.4, CH_3	3.94, s

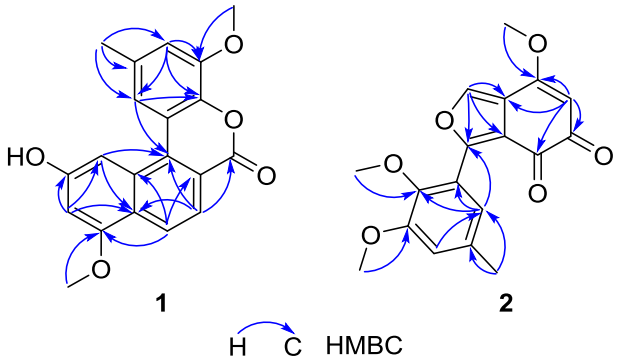

Fig. 2. Key HMBC correlations of childinins A-B (**1**–**2**).

(δ_C 123.3); H-4′ (δ_H 7.08) to C-2′, C-3′, C-6′; and H-6′ to the quaternary carbon C-1′ (δ_C 122.9), C-2′ (Fig. 2). The remaining carbons constructed an isobenzofuran system as established by HMBC correlations from H-4 (δ_H 5.90, s) to C-2 (δ_C 175.3, s), C-3 (δ_C 182.3, s), C-5 (δ_C 166.0, s), C-6 (δ_C 121.4, s) and from H-8 (δ_H 8.11, s) to C-1 (δ_C 117.4, s), C-6, C-7 (δ_C 159.4, s) (Fig. 2). The connection of the benzene ring and isobenzofuran ring between C-2 and C-10 was supported by HMBC correlation from H-6′ to C-7 (Fig. 2). Thus compound **2** was elucidated as 7-(2,3-dimethoxy-5-methylphenyl)-5-methoxyisobenzofuran-2,3-dione which shares a similar skeleton with daldinal C (Hashimoto et al., 1994; Quang et al., 2006).

The white powder childinin C (**3**) gave a molecular formula of $C_{23}H_{29}NO_5$ according to the (+)-HRESIMS ion at *m/z* 422.1940 $[M + Na]^+$ (calcd for $C_{23}H_{29}NO_5Na$, 422.1938). The ^1H NMR spectrum (Table 2) showed signals for four aromatic protons at δ 6.07 (H-6′, brs), 6.32 (H-2, brs), 6.43 (H-4, brs) and 6.62 (H-4′, brs), a methine at δ 5.86 (H-7, s), three methoxys at δ 3.68 (5-OMe), 3.86 (3′-OMe) and 3.93 (2′-OMe), and three methyls at δ 0.82 (Me-5″, d, J = 6.6 Hz), 0.83 (Me-4″, d, J = 6.6 Hz) and 2.13 (Me-7′, s). The ^{13}C NMR spectrum displayed twenty-three carbon resonances ascribable to one carbonyl carbon (δ_C 168.5, C-8), eight quaternary carbons (δ_C 111.1, 130.2, 134.6, 145.6, 151.2, 152.5, 158.3, and 162.2), four sp^2 methine carbons (δ_C 98.8, 102.6, 112.8, and 118.7), three methoxys (δ_C 55.5, 55.8, and 61.6), three methyls (δ_C 21.4, 22.4, and 22.9), two methylenes (δ_C 37.1, 38.4), and two methines (δ_C 25.8, 56.6). Preliminary analyses of these data suggested that compound **3** possesses an isoindolinone backbone, similar to that of daldinan A (Lee et al., 2012). Analyses of ^1H-^1H COSY data, as well as HMBC correlations (Fig. 3), established a 3-methylbutyl moiety, which is connected to N-9 as supported by HMBC correlations from H-1″ to C-7 and C-8. In addition, the OH at C-2′ in daldinan A is replaced by a methoxy in **3**, as supported by HMBC correlation from δ_H 3.93 (3H, s, OMe-2′) to δ_C 145.6 (s, C-2′). Detailed analyses of 2D NMR data suggested that other parts of **3** are the same to those of daldinan A (Fig. 3).

Compound **3** was determined to be racemic based on the specific rotation data (−0.3, *c* 0.45, MeOH) and chiral phase HPLC analysis result (Fig. S48, Supplementary Information). The antipodes **3a** and **3b** were separated by chiral phase HPLC, leading to the first measurements of their CD spectra and specific rotations. To establish the absolute configurations of **3a** and **3b**, the electronic circular dichroism (ECD) were calculated on the simplified structure **3s** (Supplementary Information, Pages 52–54). Overall, 19 possible conformers were generated by the MMFF94S force field conformation search (Dauria et al., 1991; Wu et al., 2016; Frisch et al., 2010), the geometries of which were further optimized by the density functional theory method at the B3LYP/6-31G(d,p) level by Gaussian 09 program package to give three predominant conformers (Goto and Osawa, 1989, 1993). These three conformers were subjected to theoretical calculation of ECD spectra by using the time-dependent DFT method at the B3LYP/6-31G(d,p) with PCM model in MeOH. As shown in Fig. 4, the calculated ECD spectra

Table 2
NMR spectroscopic data (600 MHz, C_5D_5N) for childinins B-E (**2**–**5**).

No.	**2**[a]		**3**[b]		**4**[c]		**5**[c]	
	δ_C, type	δ_H (J in Hz)	δ_C, type	δ_H (J in Hz)	δ_C, type	δ_H (J in Hz)	δ_C, type	δ_H (J in Hz)
1	117.4, C		151.2, C		140.0, C		139.4, C	
2	175.3, C		102.6, CH	6.32, brs	166.7, C		105.5, CH	6.57, brs
3	182.3, C		162.2, C		158.2, C		160.3, C	
4	103.9, CH	5.90, s	98.8, CH	6.43, brs	102.7, CH	6.62, d (2.0)	105.0, CH	6.68, brs
5	166.0, C		158.3, C		112.2, C		158.6, C	
6	121.4, C		111.1, C		109.2, CH	6.33, d (2.0)	109.2, CH	6.65, brs
7	159.4, C		56.6, CH	5.86, s	195.2, C		197.5, C	
8	141.0, CH	8.11, s	168.5, C		160.2, C			
1′	122.9, C		130.2, C		132.6, C		121.0, C	
2′	146.7, C		145.6, C		144.8, C		147.8, C	
3′	153.6, C		152.5, C		152.1, C		144.4, C	
4′	117.4, CH	7.07, brd (2.0)	112.8, CH	6.62, brs	116.5, CH	7.06, d (1.8)	115.8, CH	7.00, brs
5′	134.2, C		134.6, C		133.4, C		127.8, C	
6′	123.3, CH	7.08, brd (2.0)	118.7, CH	6.07, brs	120.5, CH	6.67, d (1.8)	124.6, CH	6.68, brs
7′	21.1, CH_3	2.34, s	21.4, CH_3	2.13, s	20.7, CH_3	2.28, s	20.6, CH_3	2.24, brs
1″			38.4, CH_2	3.89, overlap 2.73, ddd (13.8, 8.3, 5.8)				
2″			37.1, CH_2	1.40, m, 1.32, m				
3″			25.8, CH	1.48, m				
4″			22.4, CH_3	0.82, d (6.6)				
5″			22.9, CH_3	0.83, d (6.6)				
3-OMe					55.9, CH_3	3.75, s	55.3, CH_3	3.73, s
5-OMe	57.3, CH_3	4.04, s	55.5, CH_3	3.68, s	51.7, CH_3	3.56, s		
2′-OMe	56.3, CH_3	3.90, s	61.6, CH_3	3.93, s	60.8, CH_3	3.51, s		
3′-OMe	61.4, CH_3	3.75, s	55.8, CH_3	3.86, s	55.9, CH_3	3.82, s	55.9, CH_3	3.82, s

[a] Measured in acetone-d_6.
[b] Measured in $CDCl_3$.
[c] Measured in DMSO-d_6.

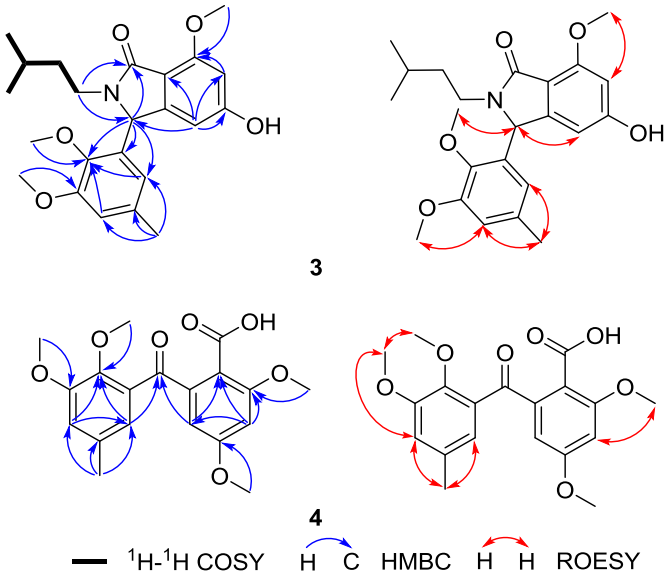

Fig. 3. Selected HMBC and ROESY correlations of childinins D and E (**3**–**4**).

for 7*R*-**3s** and 7*S*-**3s** are in good accordance with the experimental data. Thus, the absolute configurations of **3a** and **3b** are determined as 7*S* and 7*R*, respectively (Fig. 4).

The molecular formula of childinin D (**4**) was determined to be $C_{19}H_{20}O_7$ based on HRESIMS at *m/z* 383.1102 $[M + Na]^+$ (calcd for $C_{19}H_{20}O_7Na$, 383.1101), indicating ten degrees of unsaturation. The 1D NMR (Table 2) as well as HSQC spectra showed signals for two 1,2,3,5-substituted benzene rings (δ_H 6.62, 6.33 and δ_C 102.7, 109.2, 112.2, 140.0, 158.2, 112.2, 166.7; δ_H 6.67, 7.06 and δ_C 116.5, 120.5, 132.6, 133.4, 144.8, 152.1), one ketone carbonyl (δ_C 195.2), one sp^2 quaternary carbon (δ_C 160.2), four methoxys (δ_H 3.51, 3.56, 3.75, 3.82 and δ_C 60.8, 51.7, 55.9, 60.8), and one methyl singlet (δ_H 2.28 and δ_C 20.7), which share structural similarity with those of daldinal B (Quang et al., 2006; Hashimoto et al., 1994). The aldehyde group at C-2 is oxygenated to a carboxyl group (δ_C 160.2) and the hydroxy at C-5 is replaced by a methoxy in **4**. The other data were assigned carefully by HMBC and ROESY data which were in good agreement with those of daldinal B (Fig. 3).

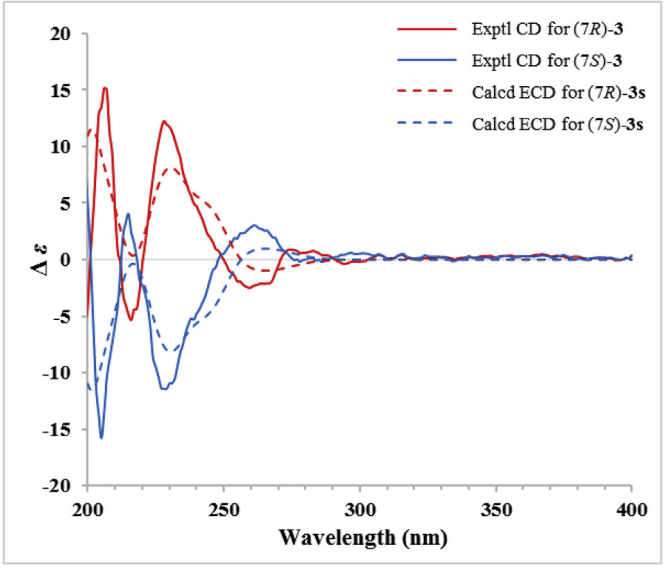

Fig. 4. Experimental CD spectra of (7*R*)- and (7*S*)-**3** and calculated ECD spectra of the simplified structure (7*R*)- and (7*S*)-**3s**.

The molecular formula of childinin E (**5**) was assigned as $C_{16}H_{16}O_5$ on the basis of HRESIMS data at *m/z* 289.1071 $[M + H]^+$ (calcd for $C_{16}H_{17}O_5$, 289.1076). The spectroscopic data of childinin E (**5**) indicated that it shares the same benzophenone backbone to that of **4** (Table 2). Detailed analyses of 2D NMR data suggested that a singlet for olefinic proton (δ_H 6.57, brs) at C-2 appears in **5** instead of the carboxyl group in **4**. In addition, the methoxy groups at C-3 and C-2′ in **4** are replaced by hydroxys in **5** (Figs S27, S28, Supplementary Information).

The molecular formula of childinin F (**6**) was $C_{12}H_{18}O_3$ based on HRESIMS at *m/z* 211.1328 $[M + H]^+$ (calcd for $C_{12}H_{19}O_3$, 211.1329). Analysis of the 1D and HSQC NMR spectra showed the presence of two methyls (δ_H 0.82, 1.82; δ_C 13.8, 9.2), one methoxy (δ_H 3.75, δ_C 56.0), four methylenes (δ_H 1.23, 1.25, 1.57, 2.43; δ_C 31.2, 22.3, 26.9, 30.8), one methine (δ_H 5.38, δ_C 87.5), and four sp^2 quaternary carbons (δ_C 106.7, 161.2, 164.8, 171.8) (Table 3). The aforementioned data suggested that the structure of **6** is similar to that of ficipyrone C (Wu et al., 2016) except that the alkyl chain is degraded by two carbons, which is supported by HMBC, ^{1}H-^{1}H COSY, and HRESIMS data. Its structure was further identified by the single crystal X-ray diffraction (Fig. 5).

HRESIMS result (*m/z* 211.1329, $[M + H]^+$) of childinin G (**7**) suggested that it is an isomer of compound **6**. It was also suggested that the structures of both compounds are almost the same by comparing the 1D NMR spectroscopic data (Table 3). The only difference was that the methyl is located at C-3 in **7** instead of at C-5 in **6**, which was supported by HMBC correlations from Me-3 (δ_H 1.90, s) to C-2 (δ_C 166.2, s), C-3 (δ_C, 94.3, s), and C-4 (δ_C 166.0, s) and from H-5 (δ_H 5.99, s) to C-6 (δ_C 164.6, s), C-7 (δ_C 34.3, t) (Fig. S40, Supplementary Information). Detailed analyses of 2D NMR data suggested that other parts of **7** are the same as those of **6**.

Compound **8** was obtained as colorless crystals (MeOH). Its molecular formula was determined as $C_{28}H_{40}O_3$ by HRESIMS at *m/z* 447.2873 $[M + Na]^+$ (calcd for $C_{28}H_{40}O_3Na$, 447.2870), corresponding to nine degrees of unsaturation. The ^{1}H NMR data showed typical signals for steroidal system: two methyl singlets at δ_H 0.91 (Me-19), 1.09 (Me-18), four methyl doublets at δ_H 1.23 (Me-21, $J = 6.7$ Hz), 0.94 (Me-28, $J = 7.0$ Hz), 0.85 (Me-26, $J = 7.0$ Hz), 0.85 (Me-27, $J = 7.0$ Hz) and two *trans* olefinic protons at δ_H 5.28 (H-22, dd, $J = 15.0$, 8.2 Hz), 5.32 (H-23, dd, $J = 15.0$, 7.4 Hz) (Table 4). The ^{13}C and DEPT NMR spectra revealed the presence of nine sp^2 carbons (3 × C=O, 1 × C=C, 1 × CH=C, 1 × CH=CH) and 19 sp^3 carbons (6 × CH_3, 6 × CH_2, 5 × CH, 2 × C) (Table 4). From the data, a tricyclic backbone is established for compound **8**. Analyses of 2D NMR spectra suggested that **8** might be an 8,14-*seco*-steroid which structurally resembles jereisteml B (Dauria et al., 1991). The key HMBC correlations from Me-18 to C-14 (δ_C 224.0), and from H-6 (δ_H 6.95, d, $J = 10.0$ Hz)/H-9 (δ_H 2.31, dd, $J = 8.3$, 1.0 Hz) to C-8 (δ_C 199.7) suggested that the keto carbons should be assigned to C-8 and C-14, respectively. The single crystal X-ray diffraction not only confirmed the structural elucidation above but also determined the absolute configuration to be 9*R*,10*R*,13*R*,17*R*,20*R*,24*R* (Fig. 6). Compound **8** was, therefore, elucidated as shown and given the name childinasterone A.

2.2. Inhibitory activities on NO production and antibacterial as well as cytotoxic activities of metabolites

All the compounds, except compound **8**, were assayed for their antibacterial activities against *Escherichia coli* ATCC 25922, *Staphylococcus aureus* subsp. *aureus* ATCC 29213, *Salmonella enterica* subsp. *enterica* ATCC 14028, and *Pseudomonas aeruginosa* ATCC 27853. The results indicated that compounds **1**, **2**, **6**, and **7** could

Table 3
NMR spectroscopic data (600 MHz, $CDCl_3$) for childinins F (**6**) and G (**7**).

No.	**6**		**7**	
	δ_C, type	δ_H (J in Hz)	δ_C, type	δ_H (J in Hz)
2	164.8, C		166.2, C	
3	87.5, CH	5.38, s	94.3, C	
4	171.8, C		166.0, C	
5	106.7, C		94.3, CH	5.99, s
6	161.2, C		164.6, s	
7	30.8, CH_2	2.43, t (7.9)	34.3, CH_2	2.47, t (7.9)
8	26.9, CH_2	1.57, m	26.9, CH_2	1.66, m
9	31.2, CH_2	1.23, overlap	31.3, CH_2	1.32, overlap
10	22.3, CH_2	1.25, m	22.5, CH_2	1.32, overlap
11	13.8, CH_3	0.82, t (7.1)	14.1, CH_3	0.89, t (7.1)
3-Me			8.6, CH_3	1.90, s
5-Me	9.2, CH_3	1.82, s		
4-OMe	56.0, CH_3	3.75, s	56.3, CH_3	3.87, s

inhibit the growth of *Staphylococcus aureus* subsp. *aureus*, *Salmonella enterica* subsp. *enterica*, *Pseudomonas aeruginosa* at the concentration 128 $\mu g \cdot mL^{-1}$, and the MIC_{90} value of **2** against *S. aureus* subsp. *aureus* was 54.9 $\mu g \cdot mL^{-1}$ (167.4 μM) (Table S1, Supplementary Information).

In addition, compounds **1** and **3**–**8** were evaluated for their inhibitory activities on NO production and cytotoxic activities. However, compound **2** was not tested for these activities due to it exhausted in the antibacterial experiment. The bioassay results showed that none of them, except compound **8**, displayed significant activities. Childinasterone A (**8**) showed inhibitory effect on NO production with an IC_{50} value of 21.2 μM, which was stronger than that of the positive control L-NMMA (IC_{50} 41.5 μM) (Table S2, Supplementary Information). Compound **8** in addition possessed weak cytotoxicity against SMMC-7721 (inhibition rate 53.3%), MCF-7 (inhibition rate 64.6%) and SW480 (inhibition rate 67.0%) at 40 μM (Table S3, Supplementary Information).

Quang Dang Ngoc et al. reported that daldinals A and B displayed significant inhibitory activities on NO production (Quang et al., 2006), whereas the activities of their analogues **6**–**7** were quite weak, indicating the substituents of aldehyde group at C-2 and/or hydroxy at C-5 were essential for this activity.

3. Conclusions

In summary, eight previously undescribed fungal metabolites (**1**–**8**) were obtained from the ascomycete *D. childiae*. Among the isolated metabolites, compound **1** has a previously undescribed 6*H*-naphtho[2,1-*c*]chromen-6-one skeleton. The specific rotatory values and Cotton effects of *R*/*S*-enantiomers of **3** were successfully and firstly assigned via ECD calculation. Based on the single crystal X-ray diffraction data of childinasterone A, the absolute configurations of the 8,14-*seco*-ergosterol skeleton were established to be 9*R*,10*R*,13*R*,17*R*,20*R*,24*R* for the first time. Bioassay results showed that childinin B (**2**) exhibited remarkable activity against *S. aureus* subsp. *aureus* with an MIC_{90} value of 54.9 $\mu g \cdot mL^{-1}$ (167.4 μM) and childinasterone A (**8**) inhibited NO production with an IC_{50} value of 21.2 μM.

4. Experimental

4.1. General experimental procedures

Optical rotations were obtained on a JASCO P-1020 digital polarimeter (Horiba, Kyoto, Japan). UV spectra were recorded on a Shimadzu UV-2401PC UV–visible recording spectrophotometer (Shimadzu, Kyoto, Japan). 1D and 2D NMR spectra were obtained on a Bruker Avance III 600 MHz spectrometer (Bruker Corporation, Karlsruhe, Germany). HRESIMS were recorded on an Agilent 6200 Q-TOF MS system (Agilent Technologies, Santa Clara, CA, USA). HREIMS were recorded on a Waters AutoSpec Premier P776 MS system. Single crystal X-ray diffraction were performed on an APEX II DUO spectrophotometer (Bruker AXS GmbH, Karlsruhe, Germany). Melting points were measured on an X-4 microscopic melting point meter (Yuhua Instrument Co., Ltd, Gongyi, China). Sephadex LH-20 (Amersham Biosciences, Uppsala, Sweden) and silica gel (Qingdao Haiyang Chemical Co., Ltd) were used for column chromatography (CC). Medium Pressure Liquid Chromatography (MPLC) was performed on a Büchi Sepacore System equipped with pump manager C-615, pump modules C-605 and fraction collector C-660 (Büchi Labortechnik AG, Flawil, Switzerland), and columns packed with Chromatorex C-18 (40–75 μm, Fuji Silysia Chemical Ltd., Kasugai, Japan). Preparative High Performance Liquid Chromatography (prep-HPLC) were performed on an Agilent 1260 liquid chromatography system equipped with Zorbax SB-C18 columns (particle size 5 μm, dimensions 9.4 mm × 150 mm or 21.2 mm × 150 mm, flow rate 10 and 20 mL min^{-1}, respectively) and a DAD detector (Agilent Technologies, Santa Clara, CA, USA). Chiral phase HPLC analysis/preparation were performed on an Agilent 1100 liquid chromatography system equipped with a Diacel CHIRAL-PAK AS-H column (particle size 5 μm, dimensions 4.6 mm × 250 mm).

4.2. Fungal material

The fungus *D. childiae* was collected from the Kunming Botanical Garden (102°44′39.50″E, 25°08′17.86″N) in July 2015. The fungus was identified by Prof. Zhu L. Yang (Kunming Institute of Botany, CAS). A voucher specimen of *D. childiae* was deposited at the Mushroom Bioactive Natural Products Research Group in Kunming

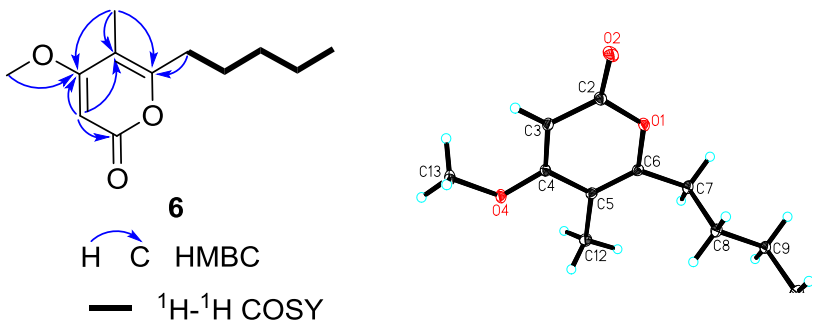

Fig. 5. ^1H-^1H COSY, key HMBC correlations and ORTEP drawing of childinin F (**6**).

Table 4
NMR spectroscopic data (600 MHz, $CDCl_3$) for childinasterone A (**8**).

No.	δ_C, type	δ_H (*J* in Hz)
1	34.0, CH_2	2.13, ddd (13.4, 5.1, 2.3) 2.01, overlap
2	33.4, CH_2	2.54, ddd (18.0, 5.7, 2.3) 2.49, ddd (18.0, 14.0, 5.1)
3	198.9, C	
4	129.3, CH	6.03, s
5	159.2, C	
6	142.3, CH	6.95, d (10.0)
7	132.5, CH	6.21, d (10.0)
8	199.7, C	
9	58.7, CH	2.31, dd (8.3, 1.0)
10	40.9, C	
11	18.0, CH_2	1.91, m
12	37.6, CH_2	1.84, ddd (12.0, 12.0, 5.1) 1.53, overlap
13	52.5, C	
14	224.8, C	
15	24.6, CH_2	2.02, overlap 1.47, overlap
16	38.1, CH_2	2.37, overlap 2.03, overlap
17	46.7, CH	2.02, overlap
18	18.9, CH_3	0.91, s
19	18.7, CH_3	1.09, s
20	39.4, CH	2.23, m
21	20.8, CH_3	1.23, d (6.7)
22	134.0, CH	5.28, dd (15.0, 8.2)
23	133.8, CH	5.32, dd (15.0, 7.4)
24	43.0, CH	1.91, overlap
25	33.2, CH	1.50, overlap
26	19.8, CH_3	0.84, d (7.0)
27	20.1, CH_3	0.86, d (7.0)
28	17.7, CH_3	0.94, d (7.0)

Institute of Botany (No. HFG 2015074).

4.3. Extraction and isolation

The powder of fresh fruiting bodies of *D. childiae* (7 kg) was macerated three times with 95% EtOH. The extract was evaporated under reduced pressure and partitioned between EtOAc and water for four times to give a EtOAc layer (45 g). The crude extract was subject to silica gel column chromatography (petroleum ether/acetone from 10:1 to 1:1 (v/v)) affording four fractions (A–D). Fraction B (5 g) was eluted on MPLC with a stepwise gradient of MeOH/H_2O (v/v 40:60-100:0) to afford fifteen subfractions (B1-B15). Subfraction B5 (0.4 g) was separated by Sephadex LH-20 (MeOH) to give eight major subfractions (B5a-B5h). Subfraction B5h was purified on prep-HPLC (MeCN/H_2O: 44.5%, isocratic, 20 mL min^{-1}, 25 min) to yield compound **1** (1.3 mg, t_R = 19.5 min). Likewise, compounds **2** (1.4 mg, MeCN/H_2O: 37%–47%, 25 min, 20 mL min^{-1}, t_R = 14.0 min), **3** (2.5 mg, MeCN/H_2O: 30%–55%, 25 min, 20 mL min^{-1}, t_R = 19.5 min), **6** (47.0 mg, MeCN/H_2O: 30%–50%, 25 min, 20 mL min^{-1}, t_R = 23.5 min), **7** (1.9 mg, MeCN/H_2O: 30%–50%, 25 min, 20 mL min^{-1}, t_R = 21.0 min), **4** (33.0 mg, MeCN/H_2O: 30%–45%, 25 min, 20 mL min^{-1}, t_R = 14.5 min), **5** (0.8 mg, MeCN/H_2O: 30%–40%, 20 min, 20 mL min^{-1}, t_R = 13.5 min) and **8** (2.4 mg, MeCN/H_2O: 50%–70%, 25 min, 10 mL min^{-1}, t_R = 22.5 min) by prep-HPLC from B8e, B9c, B8b, B8b, B7d, B7e, B14c, respectively. Compounds **3a** (1.2 mg, t_R = 11.1 min) and **3b** (1.2 mg, t_R = 25.2 min) were separated by chiral phase HPLC (*n*-hexane/isopropanol: 90%, isocratic, 30 min, 1 mL min^{-1}).

4.4. Spectroscopic data of compounds

^1H, ^{13}C, 2D NMR, and MS spectra of previously undescribed compounds (**1**–**8**) can be found in the Supplementary Information.

4.4.1. Childinin A (*1*)

Yellow powder; UV (MeOH) λ_{max} (log ε) 203.0 (4.39), 220.5 (4.30), 253.5 (4.20), 274.5 (4.19), 329.5 (3.69), 398.5 (3.48) nm; IR (KBr) ν_{max}: 3427, 1725, 1629, 1384, 1027 cm^{-1}; ^1H NMR (600 MHz, pyridine-d_5) and ^{13}C NMR (150 MHz, pyridine-d_5) data, see Table 1; HREIMS *m/z* 336.1003 $[M]^+$ (calcd for $C_{20}H_{16}O_5$, 336.0998).

4.4.2. Childinin B (*2*)

Yellow oil; UV (MeOH) λ_{max} (log ε) 206.0 (4.39), 220.5 (4.45), 273.0 (3.84), 390.5 (3.50) nm; IR (KBr) ν_{max} 1625, 1384, 1031 cm^{-1}; ^1H NMR (600 MHz, acetone-d_6) and ^{13}C NMR (150 MHz, acetone-d_6) data, see Table 2; HREIMS *m/z* 328.0941 $[M]^+$ (calcd for $C_{18}H_{16}O_6$, 328.0947).

4.4.3. (±)-Childinin C (*3*)

White powder; UV (MeOH) λ_{max} (log ε) 204.5 (4.49), 219.0 (4.38), 260.0 (3.91), 286 (3.69) nm; IR (KBr) ν_{max} 3424, 2955, 2928, 2855, 1616, 1492, 1384, 1149, 1087, 554 cm^{-1}; ^1H NMR (600 MHz, $CDCl_3$) and ^{13}C NMR (150 MHz, $CDCl_3$) data, see Table 2; HRESIMS *m/z* 422.1940 $[M + Na]^+$ (calcd for $C_{23}H_{29}NO_5Na$, 422.1938). **3a** (7*S*): [α]25D −72.29 (*c* 0.16, MeOH), CD (MeOH) λ_{max} (Δ ε): 205 (−15.8), 215 (+4.0), 229 (−11.4), 261 (+3.00); **3b** (7*R*): [α]25D +54.17 (*c* 0.12, MeOH), CD (MeOH) λ_{max} (Δ ε): 206 (+15.2), 216 (−5.3), 228 (+12.3), 259 (−2.5).

4.4.4. Childinin D (*4*)

White powder; UV (MeOH) λ_{max} (log ε): 206.0 (4.90), 221.0 (4.74), 258.0 (4.32), 315.0 (3.95) nm; IR (KBr) ν_{max} 3424, 2945, 1733, 1705, 1667, 1604, 1588, 1486, 1464, 1431, 1344, 1276,1169, 1099,

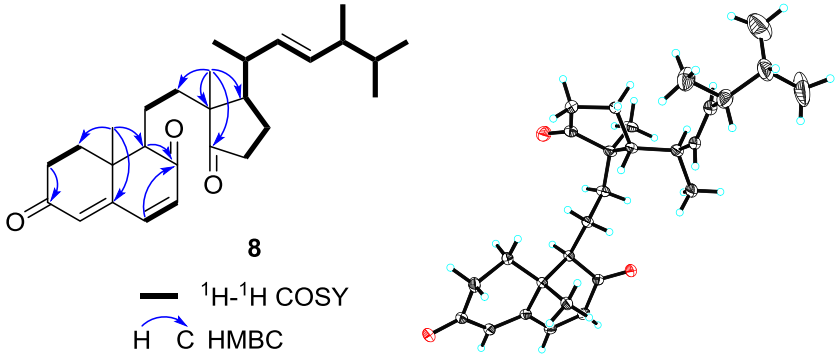

Fig. 6. Key ^1H-^1H COSY, HMBC correlations and ORTEP drawing of childinasterone A (**8**).

1022, 981 cm^{-1}; ^1H NMR (600 MHz, DMSO-d_6) and ^{13}C NMR (150 MHz, DMSO-d_6) data, see Table 2; HRESIMS *m/z* 383.1102 $[M + Na]^+$ (calcd for $C_{19}H_{20}O_7Na$, 383.1101).

4.4.5. Childinin E (**5**)

White powder; UV (MeOH) λ_{max} (log ε) 203.5 (4.53), 223.0 (4.32), 281.5 (3.98), 411.5 (3.45) nm; IR (KBr) ν_{max} 3426, 1629, 1384, 1024, 589 cm^{-1}; ^1H NMR (600 MHz, DMSO-d_6) and ^{13}C NMR (150 MHz, DMSO-d_6) data, see Table 2; HRESIMS *m/z* 289.1071 $[M + H]^+$ (calcd for $C_{16}H_{17}O_5$, 289.1071).

4.4.6. Childinin F (**6**)

Colorless needles (acetone); mp 121–123 °C; UV (MeOH) λ_{max} (log ε) 204.5 (4.40), 286 (3.83) nm; IR (KBr) ν_{max} 2957, 2932, 2863, 1721, 1647, 1566, 1457, 1407, 1345, 1247, 1126, 811 cm^{-1}; ^1H NMR (600 MHz, $CDCl_3$) and ^{13}C NMR (150 MHz, $CDCl_3$) data, see Table 3; HRESIMS *m/z* 211.1328 $[M + H]^+$ (calcd for $C_{12}H_{18}O_3$, 211.1329).

Crystal data for Mo_**6**_0m: $C_{12}H_{18}O_3$, $M = 210.26$, $a = 11.829(18)$ Å, $b = 8.373(12)$ Å, $c = 12.972(19)$ Å, $\alpha = 90°$, $\beta = 110.52(2)°$, $\gamma = 90°$, $V = 1203(3)$ $Å^3$, $T = 100(2)$ K, space group *P*21/*n*, $Z = 4$, μ(MoKα) = 0.082 mm^{-1}, 7224 reflections measured, 2693 independent reflections ($R_{int} = 0.0242$). The final R_1 values were 0.0461 ($I > 2\sigma(I)$). The final $wR(F^2)$ values were 0.1238 ($I > 2\sigma(I)$). The final R_1 values were 0.0614 (all data). The final $wR(F^2)$ values were 0.1350 (all data). The goodness of fit on F^2 was 1.110. Crystallographic data for compound **6** has been deposited at the Cambridge Crystallographic Data Center (CCDC 1532939). These data can be obtained free from the Cambridge Data Center via the link https://www.ccdc.cam.ac.uk.

4.4.7. Childinin G (**7**)

Yellow oil; ^1H NMR (600 MHz, $CDCl_3$) and ^{13}C NMR (150 MHz, $CDCl_3$) data, see Table 3; HRESIMS *m/z* 211.1329 $[M + H]^+$ (calcd for $C_{12}H_{18}O_3$, 211.1329).

4.4.8. Childinasterone A (**8**)

Colorless needles (MeOH); mp 171–174 °C; [α]25D +16.87 (*c* 0.05, MeOH); UV (MeOH) λ_{max} (log ε) 203.5 (3.86), 287.0 (4.33) nm; IR (KBr) ν_{max} 2957, 2926, 2855, 1720, 1710, 1631, 1384 cm^{-1}; ^1H NMR (600 MHz, $CDCl_3$) and ^{13}C NMR (150 MHz, $CDCl_3$) data, see Table 4; HRESIMS *m/z* 447.2873 $[M + Na]^+$ (calcd for $C_{28}H_{40}O_3Na$, 447.2870).

Crystal data for Cu_**8**_0m: $C_{28}H_{40}O_3$, $M = 424.60$, $a = 7.4765(2)$ Å, $b = 10.6607(2)$ Å, $c = 30.1431(6)$ Å, $\alpha = 90°$, $\beta = 90°$, $\gamma = 90°$, $V = 2402.55(9)$ $Å^3$, $T = 100(2)$ K, space group *P*212121, $Z = 4$, μ(CuKα) = 0.575 mm^{-1}, 16356 reflections measured, 4275 independent reflections ($R_{int} = 0.0462$). The final R_1 values were 0.0638 ($I > 2\sigma(I)$). The final $wR(F^2)$ values were 0.1683 ($I > 2\sigma(I)$). The final R_1 values were 0.0659 (all data). The final $wR(F^2)$ values were 0.1707 (all data). The goodness of fit on F^2 was 1.064. Flack parameter = 0.12 (11). Crystallographic data for compound **8** has been deposited to the Cambridge Crystallographic Data Center (CCDC 1532938).

4.5. Bioassays

4.5.1. Antibacterial assay

The tested bacteria strains *Escherichia coli* ATCC25922, *Staphylococcus aureus* subsp. *aureus* ATCC29213, *Salmonella enterica* subsp. *enterica* ATCC14028, *Pseudomonas aeruginosa* ATCC27853 were purchased from China General Microbiological Culture Collection Center, (CGMCC). All these strains were cultured in Mueller Hinton broth (MHB) (Guangdong Huankai Microbial Sci. & Tech. Co., Ltd.) at 37 °C overnight with shaking (200 rpm). A sample of each culture was then diluted 40-fold in fresh MHB broth and incubated with shaking (200 rpm) at 37 °C for 2–3 h. Compounds were first tested for their antimicrobial potential against these four strains at a single concentration of 128 μg/ml (n = 2). For those active at the single concentration of 128 μg/ml a dose response MIC (Minimum Inhibitory Concentration) assay was performed to further elucidate their activity. In this instance, bacteria were cultured in the same manner and the compounds were serially diluted two-fold across the wells of 96-well plates with concentrations ranging from 32 to 512 μg/ml, and plated in triplicate (n = 2). The resultant mid-log phase cultures were diluted to a concentration of 5×10^5 CFU/ml, then 50 μl was added to each well of the compound-containing plates, giving a final compound concentration range of 16–256 μg/ml. Plates were covered and incubated at 37 °C for 24 h. MIC_{90} was determined using photometry at $OD_{625\ nm}$. Penicillin G sodium salt (Biosharp), ceftazidime (Shanghai Yuanye Biotechnologies) were used as positive inhibitor controls.

4.5.2. Anti-NO activity

Murine monocytic RAW264.7 macrophages were dispensed into 96-well plates (2×10^5 cells/well) containing RPMI 1640 medium (Hyclone) with 10% FBS under a humidified atmosphere with 5% CO_2 at 37 °C. After 24 h of preincubation, cells were treated with serial dilutions of the test compounds, up to a maximum concentration of 25 μM (n = 2), in the presence of 1 μg/mL LPS for 18 h. The compounds were dissolved in DMSO and further diluted in medium to produce different concentrations. NO production in each well was assessed by adding 100 μL of Griess reagent (reagent A and reagent B, Sigma) to 100 μL of each supernatant from the LPS-treated or LPS- and compound-treated cells in triplicate. After 5 min incubation, the absorbance of samples was measured at 570 nm with a 2104 Envision Multilabel Plate Reader (Perkin-Elmer Life Sciences, Inc., Boston, MA, USA). MG-132 and L-NMMA were used as positive controls. Compounds **1**, **3**–**8** were tested for inhibitory activity on NO production.

4.5.3. Cytotoxicity assays

All the previously undescribed isolates except **2** were evaluated for cytotoxicity against five human cancer cell lines by MTS, an analogue of MTT method (Chen et al., 2016). The five human cancer cell lines used were HL-60 (ATCC CCL-240) human myeloid leukemia cell line, SMMC-7721 human hepatocellular carcinoma cell line, A549 (ATCC CCL-185) lung cancer cell line, MCF-7 (ATCC HTB-22) breast cancer cell line, and SW-480 (ATCC CCL-228) human colon cancer. The cell line SMMC-7721 was bought from China Infrastructure of Cell Line Resources (Beijing, China), and the remaining others from American Type Culture Collection (ATCC, Manassas, VA, USA). In these tests, DDP and taxol were used as the positive controls. Each tumor cell line was exposed to the test compound at a concentration of 40 μM in triplicates for 48 h.

Acknowledgements

This work was financially supported by National Natural Science Foundation of China (81561148013 and 81373289), the Key Projects of Technological Innovation of Hubei Province (No. 2016ACA138), and the Fundamental Research Funds for the Central University, South-Central University for Nationalities (SCUN) (CZZ17006). We thank Dr. Nana Ama Mireku-Gyimah (Department of Pharmacognosy, Faculty of Pharmacy and Pharmaceutical Sciences, Kwame Nkrumah University of Science and Technology, Ghana) for the language correction. We thank Analytical & Measuring Center, School of Pharmaceutical Sciences, SCUN, for the NMR and MS test. The computational work was supported by HPC center, Kunming Institute of Botany, CAS, China.

Appendix A. Supplementary data

Supplementary data related to this article can be found at http://dx.doi.org/10.1016/j.phytochem.2017.06.020.

References

Chang, C.W., Chein, R.J., 2011. Absolute configuration of anti-HIV-1 agent (−)-concentricolide: total synthesis of (+)-(*R*)-concentricolide. J. Org. Chem. 76, 4154–4157.

Chen, H.P., Zhao, Z.Z., Li, Z.H., Dong, Z.J., Wei, K., Bai, X., Zhang, L., Wen, C.N., Feng, T., Liu, J.K., 2016. Novel natural oximes and oxime esters with a vibralactone backbone from the basidiomycete *Boreostereum vibrans*. Chem. Open 5, 142–149.

Dauria, M.V., Paloma, L.G., Minale, L., Riccio, R., Debitus, C., 1991. Jereisterol A and jereisterol B: two 3β-methoxy-secosteroids from the Pacific sponge *Jereicopsis graphidiophora*. Tetrahedron Lett. 32, 2149–2152.

Fang, L.Z., Liu, J.K., 2009. First synthesis of racemic concentricolide, an anti-HIV-1 agent isolated from the fungus *Daldinia concentrica*. Heterocycles 78, 2107–2113.

Frisch, M.J., Trucks, G.W., Schlegel, H.B., Scuseria, G.E., Robb, M.A., Cheeseman, J.R., Scalmani, G., Barone, V., Mennucci, B., Petersson, G.A., Nakatsuji, H., Caricato, M., Li, X., Hratchian, H.P., Izmaylov, A.F., Bloino, J., Zheng, G., Sonnenberg, J.L., Hada, M., Ehara, M., Toyota, K., Fukuda, R., Hasegawa, J., Ishida, M., Nakajima, T., Honda, Y., Kitao, O., Nakai, H., Vreven, T., Montgomery Jr., J.A., Peralta, J.E., Ogliaro, F., Bearpark, M., Heyd, J.J., Brothers, E., Kudin, K.N., Staroverov, V.N., Kobayashi, R., Normand, J., Raghavachari, K., Rendell, A., Burant, J.C., Iyengar, S.S., Tomasi, J., Cossi, M., Rega, N., Millam, J.M., Klene, M., Knox, J.E., Cross, J.B., Bakken, V., Adamo, C., Jaramillo, J., Gomperts, R., Stratmann, R.E., Yazyev, O., Austin, A.J., Cammi, R., Pomelli, C., Ochterski, J.W., Martin, R.L., Morokuma, K., Zakrzewski, V.G., Voth, G.A., Salvador, P., Dannenberg, J.J., Dapprich, S., Daniels, A.D., Farkas, Ö., Foresman, J.B., Ortiz, J.V., Cioslowski, J., Fox, D.J., 2010. Gaussian 09, Revision C.01. Gaussian Inc., Wallingford, CT.

Goto, H., Osawa, E., 1989. Corner flapping: a simple and fast algorithm for exhaustive generation of ring conformations. J. Am. Chem. Soc. 111, 8950–8951.

Goto, H., Osawa, E., 1993. An efficient algorithm for searching low-energy conformers of cyclic and acyclic molecules. J. Chem. Soc. Perk. Trans. 2, 187–198.

Hashimoto, T., Tahara, S., Takaoka, S., Tori, M., Asakawa, Y., 1994. Structures of a novel binaphthyl and three novel benzophenone derivatives with plant-growth inhibitory activity from the fungus *Daldinia concentrica*. Chem. Pharm. Bull. 42, 1528–1530.

Lee, I.K., Kim, S.E., Yeom, J.H., Ki, D.W., Lee, M.S., Song, J.G., Kim, Y.S., Seok, S.J., Yun, B.S., 2012. Daldinan A, a novel isoindolinone antioxidant from the ascomycete *Daldinia concentrica*. J. Antibiot. 65, 95–97.

Qin, X.D., Dong, Z.J., Liu, J.K., Yang, L.M., Wang, R.R., Zheng, Y.T., Lu, Y., Wu, Y.S., Zheng, Q.T., 2006. Concentricolide, an anti-HIV agent from the ascomycete *Daldinia concentrica*. Helv. Chim. Acta 89, 127–133.

Quang, D.N., Harinantenaina, L., Nishizawa, T., Hashimoto, T., Kohchi, C., Soma, G.I., Asakawa, Y., 2006. Inhibitory activity of nitric oxide production in RAW 264.7 cells of daldinals A-C from the fungus *Daldinia childiae* and other metabolites isolated from inedible mushrooms. J. Nat. Med. 60, 303–307.

Wu, G., Zhou, H.C., Zhang, P., Wang, X.N., Li, W., Zhang, W.W., Liu, X.Z., Liu, H.W., Keller, N.P., An, Z.Q., Yin, W.B., 2016. Polyketide production of pestaloficiols and macrodiolide ficiolides revealed by manipulations of epigenetic regulators in an endophytic fungus. Org. Lett. 18, 1832–1835.

Zhang, A.H., Liu, W., Jiang, N., Xu, Q., Tan, R.X., 2016a. Spirodalesol, an NLRP3 inflammasome activation inhibitor. Org. Lett. 18, 6496–6499.

Zhang, A.H., Tan, R., Jiang, N., Yusupu, K., Wang, G., Wang, X.L., Tan, R.X., 2016b. Selesconol, a fungal polyketide that induces stem cell differentiation. Org. Lett. 18, 5488–5491.

Zhang, Y.L., Ge, H.M., Zhao, W., Dong, H., Xu, Q., Li, S.H., Li, J., Zhang, J., Song, Y.C., Tan, R.X., 2008. Unprecedented immunosuppressive polyketides from *Daldinia eschscholzii*, a mantis-associated fungus. Angew. Chem. Int. Ed. 47, 5823–5826.